

## Anomalous rheology of peraluminous melts

S.L. WEBB,\* E. MÜLLER, AND H. BÜTTNER

Mineralogy Department, GZG, Georg-August-University of Göttingen, Germany

### ABSTRACT

The viscosity of peraluminous  $\text{Na}_2\text{O}-\text{Al}_2\text{O}_3-\text{SiO}_2$  melts of constant  $\text{SiO}_2$  content is essentially independent of  $\text{Al}_2\text{O}_3$  content. The addition of more  $\text{Al}^{3+}$  to the peraluminous melts does not result in a decrease in viscosity. This finding indicates that the  $\text{Al}^{3+}$  in these melts does not enter the structure as a viscosity reducing network-modifier. The most probable charge-balanced structural unit in these melts is a tri-cluster that involves one Al-tetrahedron sharing an O atom with two Si-tetrahedra. Both viscosity and activation energy for viscous flow in the investigated viscosity range in these peraluminous melts are largely unaffected by the  $\text{Al}^{3+}$  content, indicating that increasing the proportion of tri-clusters does not significantly affect the mechanism of viscous flow. Comparison of data for melts of different  $\text{SiO}_2$  contents shows that the viscosity of melts in the  $\text{Na}_2\text{O}-\text{Al}_2\text{O}_3-\text{SiO}_2$  system form the same trend  $\pm 1 \log_{10}$  unit as a function of Na:Al ratio within the  $10^8$ – $10^{14}$  Pa·s range.

### INTRODUCTION

The structure of peraluminous composition melts has yet to be understood fully. The  $\text{Na}_2\text{O}-\text{Al}_2\text{O}_3-\text{SiO}_2$  system is widely used as an analog for more complex magmas. The structure of melts in this system is assumed to be made up of network-forming tetrahedrally co-ordinated  $\text{Si}^{4+}$  atoms and network-forming tetrahedrally co-ordinated  $\text{Al}^{3+}$  atoms that are charge-balanced by  $\text{Na}^+$ , with the remaining  $\text{Na}^+$  acting as network modifiers—that is, these atoms terminate a network in that they have one bond to an O atom (Mysen 1987). This description pertains to peralkaline compositions ( $\text{Na}/\text{Al} > 1$ ). If the melt composition is changed by decreasing the number of  $\text{Na}^+$  ions, there comes a stage where all of the  $\text{Na}^+$  are used to charge balance the tetrahedrally co-ordinated  $\text{Al}^{3+}$ . At this subaluminous join ( $\text{Na}/\text{Al} = 1$ ), the network should be fully polymerized, based upon the above structural model. With a further decrease in the amount of  $\text{Na}^+$ , the question is what happens to the structure of the melt and its rheology? The two extremes of structure available to the “excess” Al (that which has no  $\text{Na}^+$  to charge-balance it in tetrahedral co-ordination) are that it acts as a network-modifier in octahedral co-ordination (Mysen et al. 1981; Mysen 1988), or that it continues to occur as a tetrahedrally co-ordinated network-former in the form of “tri-clusters” (Lacy 1963) in which one O atom is the apex of two  $\text{Si}^{4+}$  tetrahedra and one  $\text{Al}^{3+}$  tetrahedron. This Na-free tri-cluster is a charge-balanced fully polymerized structural unit.

Within the framework of this structural model, it is expected that there is a maximum in viscosity for melts of constant mol%  $\text{SiO}_2$  at  $\text{Na}/\text{Al} = 1$ , as this composition is the point of maximum average bond strength and minimum configurational entropy of the melt (Toplis et al. 1997a). This is the composition at which all of the network-modifying Na atoms are used to charge-balance the Al-tetrahedra. On the peralkaline side of this composition, there is an increasing number of network-modifying  $\text{Na}^+$ , and on the peraluminous ( $\text{Na}/\text{Al} < 1$ ) side, there are increasing amounts of

either network-modifying  $\text{Al}^{3+}$  or some other structural unit that results in the charge balance of the tetrahedrally co-ordinated  $\text{Al}^{3+}$  cations. The changes in viscosity that result from the necessary changes in structure as a function of Na:Al have been observed by several authors. The data of Riebling (1966, 1968) show a maximum in viscosity (in the range  $10^1$ – $10^2$  Pa s) for  $0.45 < \text{Na}_2\text{O}/(\text{Na}_2\text{O} + \text{Al}_2\text{O}_3) < 0.50$  for melts of constant  $\text{SiO}_2$  content in the range 50–75 mol%  $\text{SiO}_2$ . Taylor and Rindone (1970) found in the  $10^9$ – $10^{13}$  Pa s range that viscosity increased with decreasing peralkalinity and then remained essentially constant with increasing peraluminosity for melts with 75 mol%  $\text{SiO}_2$ . Hunold and Brückner (1980) combined rotation viscometry with micro-penetration techniques and investigated the viscosity of melts with 66.7 mol%  $\text{SiO}_2$  across the  $10^1$ – $10^{13}$  Pa·s range and found a shallow maximum occurring for Al-rich melts at  $\text{Na}_2\text{O}/(\text{Na}_2\text{O} + \text{Al}_2\text{O}_3) \sim 0.45$ . The maximum was more pronounced for the high viscosity measurements (see Fig. 1).

More recently, Toplis et al. (1997a, 1997b) determined the viscosity of several  $\text{Na}_2\text{O}-\text{Al}_2\text{O}_3-\text{SiO}_2$  melts with  $\text{SiO}_2 \geq 50$  mol%, and observed the maximum in viscosity to occur in the slightly peraluminous compositions. They found the Na:Al ratio at which the maximum in viscosity occurs to be dependent upon the  $\text{SiO}_2$  content, and also upon temperature. Toplis et al. (1997a) interpreted their results to be consistent with a melt structure containing a proportion of tri-clusters in which one three-coordinated O atom shares an aluminate and two silicate tetrahedra. The existence of this charge balanced tri-cluster results in the presence of non-bridging O atoms bonded to  $\text{Na}^+$  in slightly peraluminous compositions (as observed in NMR studies; e.g., Stebbins and Xu 1997; Stebbins et al. 2001). The presence of octahedrally co-ordinated  $\text{Al}^{3+}$  acting as network-modifying cations would also result in a decrease in viscosity with increasing peraluminosity, and thus also explain the maximum observed in viscosity at  $\text{Na}/\text{Al} \sim 1$ . However, as pointed out by Toplis et al. (1997a), the maximum in viscosity occurs for the most peraluminous composition at 67 mol%  $\text{SiO}_2$ , and the clusters of four  $\text{Al}^{3+}$  required when one  $\text{Al}^{3+}$  acts as a charge

\* E-mail: swebb@gwdg.de

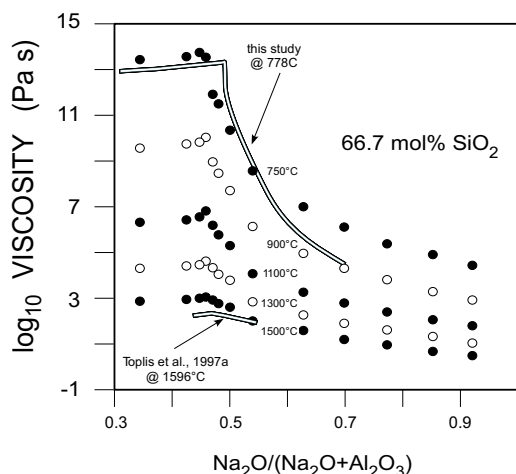


**FIGURE 1.** Viscosity data for  $\text{Na}_2\text{O}$ - $\text{Al}_2\text{O}_3$ - $\text{SiO}_2$  melts (with 66.7 mol%  $\text{SiO}_2$ ) from Hunold and Brückner (1980) plotted as a function of  $\text{Na}_2\text{O}/(\text{Na}_2\text{O} + \text{Al}_2\text{O}_3)$  for temperatures from 750 to 1500 °C, together with the trend of the present data at 778 °C, and the trend of the viscosity data of Toplis et al. (1997a) at 1596 °C.

balancer for the other three would not result in this maximum deviation at 67 mol%  $\text{SiO}_2$ . Therefore it appears that the structure of peraluminous composition melts contains  $\text{AlSi}_2\text{O}_{5.5}$  tri-clusters rather than octahedrally co-ordinated  $\text{Al}^{3+}$ . As pointed out by Toplis et al. (1997a), their data cannot, however, be used to infer the presence or absence of octahedral Al in more highly peraluminous compositions.

To address the further possible changes in melt structure with increasing alumina content, the viscosity of several  $\text{Al}_2\text{O}_3$ - and also  $\text{Na}_2\text{O}$ -rich melts with 66.7 mol%  $\text{SiO}_2$  content were determined by the micro-penetration technique.

## EXPERIMENTAL METHODS

Ten samples were made from  $\text{Na}_2\text{CO}_3$ ,  $\text{Al}_2\text{O}_3$  and  $\text{SiO}_2$  powders. The powdered mixtures were homogenized by agitation in plastic bottles, de-carbonated in Pt-crucibles at 700 °C for 12 hours, and melted at temperatures between 1250 and 1600 °C. The Na-rich samples were melted at the lower temperatures. The peraluminous melts were stirred with a Pt-stirrer at 1600 °C for 12 hours to remove the bubbles. The melts were cooled slowly (2 °C/min) through the interval between 900 and 600 °C to minimize thermal stresses. The bubble-free samples were then cored out of the crucible with a diamond borer and 3 mm thick, 8 mm diameter discs were cut for the viscosity measurements. The parallel faces of the discs were polished before the viscosity measurements. The compositions of the ten glasses (see Table 1) were determined by electron microprobe analysis. The samples were found to be crystal-free based on both optical microscopy and the surfaces observed during the microprobe measurements.

The micropenetration technique was used to determine viscosity in the range  $10^8$ – $10^{14.5}$  Pa·s. Shear viscosities for several silicate melt compositions have been determined in previous studies using the micro-penetration technique (e.g., Douglas et al. 1965; Brückner, and Demharter 1975). Viscosity was measured with a Netzsch TMA 402 Dilatometer. The rate at which a 2 mm diameter single crystal sphere of  $\text{Al}_2\text{O}_3$  is forced into the melt is measured, and viscosity is calculated by:

$$\eta = \frac{0.1875 F t}{r^{0.5} l^{1.5}} \quad (1)$$

for  $F$  = the applied force,  $t$  = time,  $r$  = radius of the sphere and  $l$  = indent distance. A typical plot of calculated viscosity as a function of time is shown in Figure 2. Masses between 50 and 500 g were used to apply the force for indent times from 15 minutes to 12 hours. The sample temperature within the dilatometer was calibrated to within  $\pm 0.5$  °C from the melting points of Ag (961.8 °C), Al (660.3 °C), Sb (630.6 °C)

**TABLE 1.** Glass compositions (mol%) determined by microprobe (JEOL JXA 8900 RL): 15 kV voltage, 10  $\mu\text{m}$  beam diameter, and 12 nA current

	$\text{SiO}_2$	$\text{Na}_2\text{O}$	$\text{Al}_2\text{O}_3$	Wt% total	$\text{Na}_2\text{O}$ $\text{Na}_2\text{O} + \text{Al}_2\text{O}_3$	$\text{Na}_2\text{O}$ wt% AAS
67:36	68.52 $\pm$ 0.41 (58.51)	11.37 $\pm$ 0.49 (10.01)	20.11 $\pm$ 0.17 (29.14)	97.64	36.1 $\pm$ 1.1	9.36 $\pm$ 0.06
67:40.3	68.23 $\pm$ 0.31 (58.70)	12.82 $\pm$ 0.30 (11.38)	18.95 $\pm$ 0.20 (27.67)	97.74	40.3 $\pm$ 0.7	10.83 $\pm$ 0.05
67:40.4	66.85 $\pm$ 0.23 58.10	13.39 $\pm$ 0.12 12.00	19.76 $\pm$ 0.11 29.14	99.24	40.4 $\pm$ 0.1	11.74 $\pm$ 0.07
67:47	67.64 $\pm$ 0.27 (59.10)	15.31 $\pm$ 0.25 (13.80)	17.05 $\pm$ 0.13 (25.28)	98.17	47.3 $\pm$ 0.5	14.40 $\pm$ 0.06
67:48	67.19 $\pm$ 0.26 (58.89)	15.95 $\pm$ 0.28 (14.42)	16.86 $\pm$ 0.15 (25.07)	97.38	48.6 $\pm$ 0.4	15.17 $\pm$ 0.05
67:49	64.97 $\pm$ 0.17 (56.22)	17.19 $\pm$ 0.16 (15.34)	17.84 $\pm$ 0.17 (26.20)	97.75	49.1 $\pm$ 0.4	15.01 $\pm$ 0.11
67:51	66.70 $\pm$ 0.28 (58.69)	16.95 $\pm$ 0.38 (15.39)	16.35 $\pm$ 0.18 (24.41)	98.48	50.9 $\pm$ 0.8	16.21 $\pm$ 0.05
67:58	69.93 $\pm$ 0.56 63.32	17.38 $\pm$ 0.36 16.24	12.69 $\pm$ 0.22 19.52	99.07	57.8 $\pm$ 0.2	18.20 $\pm$ 0.13
67:59	67.52 $\pm$ 0.97 (60.54)	19.30 $\pm$ 1.14 (17.85)	13.18 $\pm$ 0.24 (20.05)	98.44	59.4 $\pm$ 2.0	18.55 $\pm$ 0.06
67:70	67.28 $\pm$ 0.19 62.16	22.93 $\pm$ 0.17 21.85	9.79 $\pm$ 0.04 15.36	99.38	70.1 $\pm$ 0.1	22.48 $\pm$ 0.06

Notes: Data are the average of 10 analyses of each glass. Errors are 1 $\sigma$  values. The numbers in brackets are the wt% values. The  $\text{Na}_2\text{O}/(\text{Na}_2\text{O} + \text{Al}_2\text{O}_3)$  values calculated from the microprobe data are in percentages. The  $\text{Na}_2\text{O}$  determined by atomic absorption spectroscopy are also given in wt%.

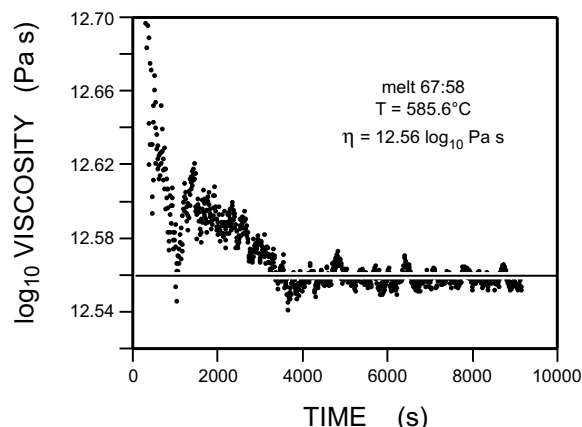


**FIGURE 2.** Viscosity calculated as a function of time for melt 67:58, for an applied force of 1.303 N. The black line is the fit to the data.

and Zn (419.5 °C) determined for heating rates from 1 to 10 °C/min. The viscosity of the standard glass DDG1 from the Deutsche Glastechnische Gesellschaft was determined to within 0.05  $\log_{10}$  Pa·s or better for viscosities between  $10^{9.2}$  and  $10^{12.5}$  Pa·s. The viscosity was also shown to be independent of the force applied, with the same viscosity (within  $\pm 0.02 \log_{10}$  Pa·s) being determined for forces of 0.2 to 4.5 N. Based upon the precision and accuracy of these calibrations, 1 $\sigma$  error of 0.06  $\log_{10}$  Pa·s is assigned to each viscosity determination. As these melts are highly viscous, some of the data were collected over a 12 hour period with the unrelaxed penetration data being discarded. In general, relaxed penetration data were obtained 3 $\tau$  after the application of the load, where  $\tau$  is the relaxation time calculated from the Maxwell equation [ $\tau$  = (viscosity)/(elastic shear modulus)].

## RESULTS

The measured viscosities as a function of temperature are in Table 2 and Figure 3. The error in each viscosity determination is  $\pm 0.06 \log_{10}$  Pa·s. Over the  $\sim 200$  °C temperature range of the

**TABLE 2.** The  $\log_{10}$  viscosity measured at each temperature

67:36		67:40.3		67:40.4		67:47		67:48	
$T$ (°C)	$\log_{10} \eta$ (Pa s)	$T$ (°C)	$\log_{10} \eta$ (Pa s)	$T$ (°C)	$\log_{10} \eta$ (Pa s)	$T$ (°C)	$\log_{10} \eta$ (Pa s)	$T$ (°C)	$\log_{10} \eta$ (Pa s)
746.2	13.84	773.0	13.17	799.7	12.43	762.5	13.63	762.5	13.67
772.8	13.17	834.7	11.61	834.7	11.61	781.1	13.20	803.8	12.68
830.6	11.65	870.7	10.72	886.2	10.42	803.8	12.57	839.8	11.73
868.7	10.71	906.8	9.89	906.8	9.93	844.9	11.42	877.8	10.74
906.8	9.83	947.8	9.04	927.3	9.47	881.0	10.64	906.8	10.11
989.0	8.31	989.0	8.36	937.6	9.21	906.8	10.07	968.5	8.90
				974.6	8.42	947.8	9.32		
						989.1	8.57		
67:49		67:51		67:58		67:59		67:70	
$T$ (°C)	$\log_{10} \eta$ (Pa s)	$T$ (°C)	$\log_{10} \eta$ (Pa s)	$T$ (°C)	$\log_{10} \eta$ (Pa s)	$T$ (°C)	$\log_{10} \eta$ (Pa s)	$T$ (°C)	$\log_{10} \eta$ (Pa s)
773.0	13.56	711.2	12.82	585.6	12.56	553.7	13.71	476.1	14.47
809.0	12.55	752.3	11.76	585.6	12.61	564.0	13.38	500.4	13.30
839.8	11.70	793.4	10.80	618.6	11.40	587.7	12.31	529.9	11.95
881.0	10.69	829.5	10.02	639.1	10.75	602.1	11.86	563.0	10.90
906.8	10.06	868.7	9.26	650.5	10.40	618.0	11.05	587.2	9.88
958.1	8.99	901.6	8.67	660.8	10.11	643.3	10.36	617.7	8.93
				670.0	9.80	673.0	9.51	637.9	8.49
				680.3	9.51	706.0	8.86		
				690.6	9.26				
				700.9	9.01				
				711.2	8.78				

Notes: The  $1\sigma$  error in viscosity is  $\pm 0.06 \log_{10}$  Pa s. The melt compositions are indicated by the  $\text{Na}_2\text{O}/(\text{Na}_2\text{O} + \text{Al}_2\text{O}_3)$  value.

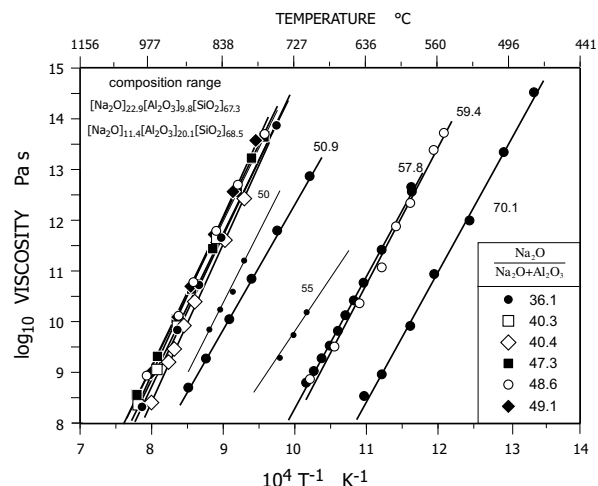


**FIGURE 3.** Viscosity of  $\text{Na}_2\text{O}-\text{Al}_2\text{O}_3-\text{SiO}_2$  melts as a function of inverse temperature. The  $1\sigma$  error in viscosity is less than the size of the symbols. The small dots are the data from Toplis et al. (1997a) for their melts 67:50 and 67:55. The  $\text{Na}_2\text{O}/(\text{Na}_2\text{O} + \text{Al}_2\text{O}_3)$  values are determined from the microprobe data.

present measurements, the data in Figure 3 are best fit by an Arrhenius equation:

$$\log_{10} \eta \text{ (Pa s)} = A + \frac{B \times 10^4}{T} \quad (2)$$

with the resulting parameters and their standard deviation presented in Table 3. Arrhenian fits to the micropenetration viscosity data of Toplis et al. (1997a, 1997b) were calculated to compare their data with that of the present study. These fit parameters are also included in Table 3. There are large errors in the activation energy term determined from the data of Toplis et al. (1997a, 1997b) as they have four or fewer data points in this high viscosity range. There appears to be a general trend that the

**TABLE 3.** Parameters fit to Equation 2 together with the activation energy for viscous flow for each composition.

Melt	$\frac{\text{Na}_2\text{O}}{\text{Na}_2\text{O} + \text{Al}_2\text{O}_3}$	A-value ( $\log_{10}$ Pa s)	B-value (K)	Activation energy (kJ mol <sup>-1</sup> )
67:36	0.361	$-15.86 \pm 0.22$	$3.03 \pm 0.02$	$581 \pm 5$
67:40.3	0.403	$-15.29 \pm 0.33$	$2.98 \pm 0.04$	$570 \pm 7$
67:40.4	0.404	$-16.13 \pm 0.41$	$3.07 \pm 0.05$	$588 \pm 10$
67:44 <sup>1a</sup>	0.441	$-19.44 \pm 4.82$	$3.43 \pm 0.55$	$657 \pm 106$
67:47 <sup>1b</sup>	0.470	$-19.78 \pm 3.62$	$3.50 \pm 0.42$	$669 \pm 80$
67:47	0.473	$-14.97 \pm 0.38$	$2.96 \pm 0.04$	$567 \pm 8$
67:48	0.486	$-15.51 \pm 0.43$	$3.03 \pm 0.05$	$580 \pm 9$
67:49	0.491	$-16.96 \pm 0.18$	$3.19 \pm 0.02$	$611 \pm 4$
67:50 <sup>1b</sup>	0.492	$-14.54 \pm 2.30$	$2.76 \pm 0.25$	$529 \pm 49$
67:51	0.509	$-12.83 \pm 0.17$	$2.52 \pm 0.02$	$483 \pm 3$
67:55 <sup>1b</sup>	0.548	$-14.30 \pm 0.89$	$2.41 \pm 0.09$	$461 \pm 17$
67:58	0.578	$-17.61 \pm 0.30$	$2.59 \pm 0.03$	$496 \pm 6$
67:59	0.594	$-18.56 \pm 1.07$	$2.66 \pm 0.09$	$509 \pm 18$
67:70	0.701	$-19.54 \pm 0.67$	$2.54 \pm 0.05$	$486 \pm 10$

Notes: The errors are the standard deviation to the fit parameters. Ta = data from Toplis et al. 1997a; Tb = data from Toplis et al. 1997b.

activation energy is larger for the peraluminous compositions. As can be seen in Figure 3, the viscosity of peralkaline composition melts increases with increasing  $\text{Al}_2\text{O}_3$  content for  $0.50 < \text{Na}_2\text{O}/(\text{Na}_2\text{O} + \text{Al}_2\text{O}_3) < 0.70$ . However, once the melt becomes peraluminous, the viscosity appears not to change—despite the addition of more  $\text{Al}_2\text{O}_3$  for melts with  $0.36 < \text{Na}_2\text{O}/(\text{Na}_2\text{O} + \text{Al}_2\text{O}_3) < 0.49$ .

## DISCUSSION

To address the variation in viscosity as a function of melt structure and Na:Al value, the present viscosity data are plotted at 778 °C as a function of  $\text{Na}_2\text{O}/(\text{Na}_2\text{O} + \text{Al}_2\text{O}_3)$  in Figure 4. The viscosity data of Toplis et al. (1997a) at this temperature are also included in Figure 4. For seven of the present melts, this plot requires no extrapolation beyond the measured temperature range. For the three  $\text{Na}_2\text{O}$ -rich samples, this plot requires a 70 to 140 °C extrapolation in temperature, which is equivalent to a  $\sim 4 \log_{10}$  unit extrapolation in viscosity. Using the data from Toplis et

al. (1997a) for their melt 67:55, it is found that such an Arrhenian extrapolation will underestimate the actual viscosity by 1  $\log_{10}$  Pa s. Extrapolation of the Arrhenian fit to the present data for melt 67:70 to 750 °C underestimates the viscosity measured by Hunold and Brückner (1980) by 0.8  $\log_{10}$  Pa s; while extrapolations of the Arrhenian curve for melts 67:58 and 67:59 plot within error of the Hunold and Brückner data at 750 °C.

The general trend in viscosity data observed in Figure 4 is essentially independent of temperature: the viscosity of the peralkaline melts is low and increases as the Na = Al join is approached, and then remains essentially unchanged as the melts become more peraluminous. As pointed out by Hunold and Brückner (1980) and Toplis et al. (1997a, 1997b), the difference in viscosity as a function of composition is minimal at high temperatures, and more extreme at the low-temperature, high-viscosity conditions of this study (see Fig. 1). The data in Figure 4 show a weak maximum in viscosity at  $\text{Na}_2\text{O}/(\text{Na}_2\text{O} + \text{Al}_2\text{O}_3) \sim 0.49$ . As observed by Toplis et al. (1997a), this maximum occurs on the peraluminous side of the composition range, which they interpreted to indicate the presence of tri-clusters in the melt structure in the vicinity of the subaluminous join. Figure 4 shows there is a plateau ( $\pm 1 \log_{10}$  Pa·s) in viscosity with increasing peraluminosity. The occurrence of this plateau indicates that  $\text{Al}^{3+}$  does not exist in these peraluminous melts in a network-modifying role, as this would result in a decrease in viscosity similar to that observed for increasingly peralkaline melts. In contrast to the study of Toplis et al. (1997a), in which the maximum in viscosity as a function of composition was determined from a 0.6  $\log_{10}$  Pa·s change in viscosity, the present study is concerned with large changes in viscosity. The  $\pm 1 \log_{10}$  Pa·s variation for the peraluminous compositions appears as a “constant” viscosity, in comparison to the  $\sim 8 \log_{10}$  Pa·s change in viscosity occurring for the peralkaline compositions (see Fig. 4).

The current perception of melt structure is based upon tetrahedrally bonded  $\text{Si}^{4+}$ , and tetrahedrally bonded  $\text{Al}^{3+}$  charge-balanced by an  $\text{Na}^+$ , with the excess  $\text{Na}^+$  in peralkaline compositions bonded to non-bridging O atoms (Lacy 1963; Mysen 1988). This model, however, breaks down when there is more  $\text{Al}^{3+}$  than charge-balancing cations, that is, for peraluminous

compositions. Peraluminous melts require a different structure model. One possibility is that  $\text{Al}^{3+}$  becomes a network modifier, which would result in a decrease in viscosity for peraluminous melts with increasing amounts of alumina. However, the present data, as well as the low-viscosity data of Riebling (1966, 1968) and the high- and low-viscosity data of Hunold and Brückner (1980), show no decrease in viscosity with increasing Al-content in peraluminous composition melts. The relatively constant, composition-independent viscosity for the peraluminous melts indicates that there are no new non-bridging O atoms being created in the structure as the melt becomes more Al rich. This “constant” viscosity also would suggest that the average bond strength and configurational entropy of the melt does not change appreciably as the melt composition becomes more Al rich (Toplis et al. 1997a).

Lacy (1963) and Toplis et al. (1997a) (as well as many others) discussed the possible structure of peraluminous melts and concluded that tri-clusters of one Al-tetrahedron and two Si-tetrahedra all sharing one O atom are the most probable structure in slightly peraluminous melts. Such a tri-cluster is charge-balanced. Toplis et al. (1997a) pointed out that the existence of the local maximum in viscosity on the peraluminous side of the composition range supports the existence of  $\text{AlSi}_2\text{O}_{5.5}$  tri-clusters. The chemically induced creation of a tri-cluster does not require the polymerization (time average of the number of bridging and non-bridging O atoms) of the melt to change. The removal of one  $\text{Na}_2\text{O}$  from a fully polymerized peraluminous melt results in the creation of two tri-clusters; but no new non-bridging O atoms are required. Similar scenarios in which the polymerization remains unaffected and tri-clusters are formed can be developed for the combined removal of a  $\text{NaO}_{0.5}$  and addition of an  $\text{AlO}_{1.5}$ , or the simple addition of one  $\text{Al}_2\text{O}_3$ .

Figure 5 shows the viscosity of a range of  $\text{Na}_2\text{O}-\text{Al}_2\text{O}_3-\text{SiO}_2$  melts with  $50 \leq \text{SiO}_2 \text{ mol\%} \leq 82$  at 778 °C. All of these data fall within  $\pm 1 \log_{10}$  unit of the same trend seen in Figure 4. Thus, in this simple ternary system, the viscosity can be estimated within  $\pm 1 \log_{10}$  Pa·s in terms of the  $\text{Na}_2\text{O}:\text{Al}_2\text{O}_3$  ratio, independent of the  $\text{SiO}_2$  content. Trends similar to that of Figure 4 can be calculated

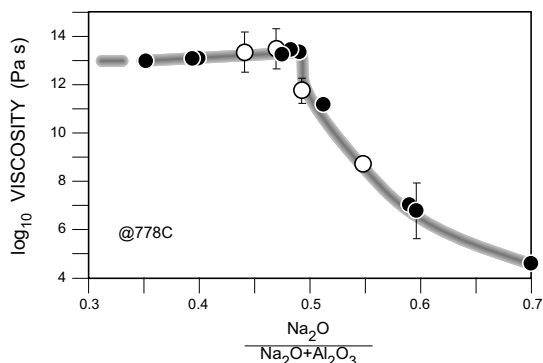


**FIGURE 4.** Viscosity data at 778 °C = filled symbols. The open symbols are the viscosity calculated at this temperature from Arrhenian fits to the micropenetration data of Toplis et al. (1997a). Unless otherwise indicated, the error in viscosity is less than the size of the symbol. The grey curve is a guide to the eye.

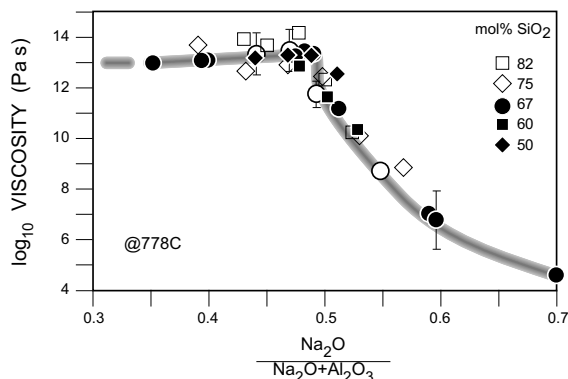


**FIGURE 5.** Viscosity of a range of  $\text{Na}_2\text{O}-\text{Al}_2\text{O}_3-\text{SiO}_2$  melts with varying  $\text{SiO}_2$  content at 778 °C; solid circles = present data; all other symbols are data from Toplis et al. (1997a, 1997b). They grey curve is the same as drawn in Figure 4.

for other temperatures, which, however, involves extrapolation of several sets of viscosity data beyond the  $10^8$ – $10^{14.5}$  Pa·s range that is described by the present Arrhenian fits. This procedure would involve increasingly larger errors in the extrapolated viscosities. Figure 6 illustrates that Na-aluminosilicate melts with  $50 \leq \text{SiO}_2$  mol%  $\leq 82$ , and  $\text{Na}_2\text{O} = \text{Al}_2\text{O}_3$  have viscosities within  $\pm 1 \log_{10}$  Pa·s of that for the jadeite composition at all temperatures. Figure 7 illustrates the same set of viscosity data together with other literature data now plotted as a function of NBO/T. The NBO/T is calculated from:

$$\frac{\text{NBO}}{T} = \frac{2(\text{Na}_2\text{O}-\text{Al}_2\text{O}_3)}{2\text{Al}_2\text{O}_3+\text{SiO}_2} \quad (3)$$

assuming no tri-clusters exist, where the components are in mole fractions of the oxides (Mysen 1987). For the melt compositions that do not have enough  $\text{Na}^+$  to charge-balance the  $\text{Al}^{3+}$ , which are assumed to be in tetrahedral coordination, this calculation gives negative NBO/T values. If tri-clusters, or some other structure that does not create non-bridging O atoms exist in these peraluminous melts, the negative NBO/T values would become equal to zero. The data in Figures 5 and 7 suggest that viscosity of  $\text{Na}_2\text{O}-\text{Al}_2\text{O}_3-\text{SiO}_2$  melts is a simple function of the degree of polymerisation of the melt structure. The Arrhenian activation energy for viscous flow at  $10^{12}$  Pa·s in the present  $\text{Na}_2\text{O}-\text{Al}_2\text{O}_3-\text{SiO}_2$  melts with 67 mol%  $\text{SiO}_2$  is plotted as a function of  $\text{Na}_2\text{O}/(\text{Na}_2\text{O} + \text{Al}_2\text{O}_3)$  in Figure 8. There appears to be a general trend of low activation energy ( $\sim 480$  kJ/mol) for  $\text{Na} > \text{Al}$ , and high activation energy ( $\sim 560$  kJ/mol) for viscous flow for  $\text{Al} > \text{Na}$ . Although there are large errors ( $\pm 50$  kJ/mol) in activation energy from the literature, based upon the low-temperature viscosity data of Poole and Gensamer (1949), Taylor and Rindone (1970), and Toplis et al. (1997a, 1997b), the activation energy also appears to be independent of  $\text{SiO}_2$  content. A similar trend

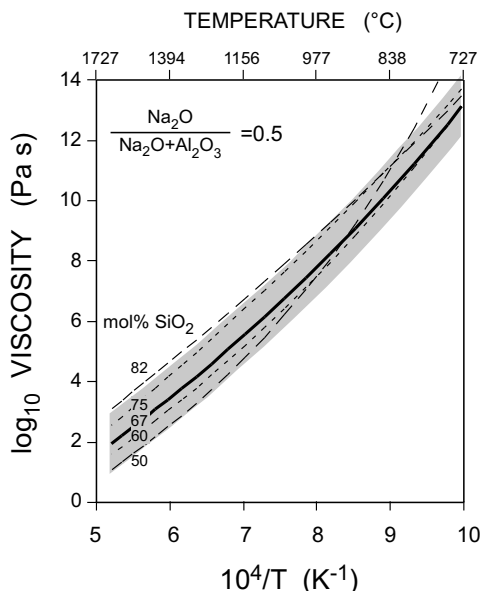


**FIGURE 6.** The viscosity of  $\text{Na}_2\text{O}-\text{Al}_2\text{O}_3-\text{SiO}_2$  melts with  $\text{Na} = \text{Al}$ . Data from Toplis et al. (1997a, 1997b). The shaded area indicates  $\pm 1 \log_{10}$  Pa s centred on the viscosity of the melt with 67 mol%  $\text{SiO}_2$ .

in activation energy as a function of composition is seen in the data of Riebling (1966, 1968) for the low-viscosity range for melts with  $50 < \text{SiO}_2$  mol%  $< 75$ .

Toplis (1998) showed that within the framework of the Adam-Gibbs theory of viscosity, the ratio of the parameters  $B_c$  (temperature independent constant) to  $S_c(T_g)$  (configurational entropy at the temperature where viscosity is  $10^{12}$  Pa·s) is proportional to the height of the average potential energy barrier to viscous flow (assuming the size of the rearranging structural domains at this temperature is a constant for all silicate melt compositions). The term  $B_c/S_c(T_g)$  is linearly proportional to the activation energy term calculated for the present melts using the Arrhenius equation. The constant value of activation energy for the present peraluminous melts (see Fig. 8) would suggest, therefore, that the mechanism of viscous flow in these melts

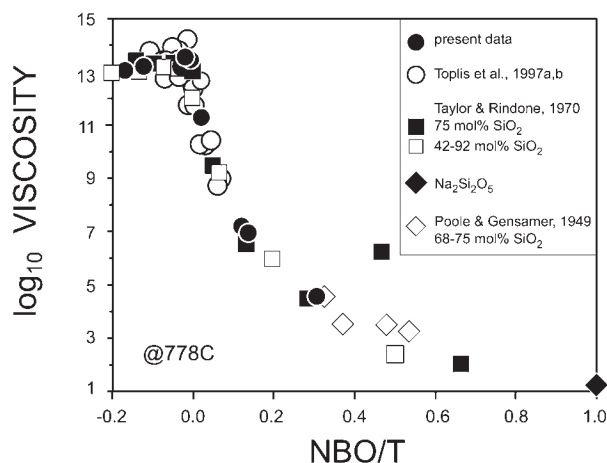


**FIGURE 7.** Viscosity of a range of  $\text{Na}_2\text{O}-\text{Al}_2\text{O}_3-\text{SiO}_2$  melts at  $778^\circ\text{C}$  as a function of NBO/T. In this case, negative values of non-bridging O atoms are calculated to illustrate the need for a change in melt structure. Data that plot below  $10^8$  Pa·s involve the extrapolation of Arrhenian fits to high-viscosity data and are thus increasingly larger ( $>1 \log_{10}$  unit) underestimates of the real viscosity.

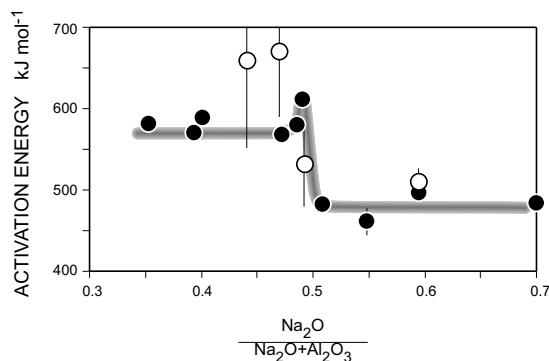


**FIGURE 8.** Activation energy from Arrhenian fits to the viscosity data. Unless otherwise indicated, the  $1\sigma$  errors are less than the size of the symbols. The open symbols are from fits to the data of Toplis et al. (1997a, 1997b). There are large errors in these energy values as only three or four data exist at these low temperatures.



does not change with increasing amounts of  $\text{Al}^{3+}$ , nor with the increasing proportions of the structure that  $\text{Al}^{3+}$  takes up in these peraluminous compositions. Similarly it can be argued that the constant activation energy for the peralkaline melts with 67 mol%  $\text{SiO}_2$  indicates that the mechanism of viscous flow is unaffected by increasing amounts of non-bridging O atoms that accompany an increase in  $\text{Na}^+$  content. The jump from low activation energy for viscous flow in peralkaline melts to higher activation energies in peraluminous melts would, however, suggest that the mechanism of viscous flow between the two compositions changes from (1) a mechanism in which weak O-Na bonds are broken in order for flow to occur in peralkaline melts to (2) a mechanism in which stronger O-Al bonds need to be broken for flow to occur in peraluminous melts (McMillan et al. 1994; Stebbins 1995; Toplis 1998).

The trend in viscosity with  $\text{Na}_2\text{O}:\text{Al}_2\text{O}_3$  ratio has not been appreciated previously, as most geological systems have a more complex chemistry. As shown in Figure 9, a similar trend may occur in mixed alkali melts. A very different pattern of viscosity as a function of composition (and NBO/T) appears for the alkaline earth compositions. There is limited data for these compositions in the peraluminous range and therefore it is not possible to determine whether there is also a plateau in viscosity for the peraluminous alkaline earth compositions.

### CONCLUDING REMARKS

Viscosity measurements for a wide range of  $\text{Na}_2\text{O}-\text{Al}_2\text{O}_3-\text{SiO}_2$  composition melts shows that there is not a maximum in viscosity in the vicinity of the Na = Al composition, rather, there is a plateau in viscosity for peraluminous melts. Thus, the  $\text{Al}^{3+}$  replacing  $\text{Na}^+$  in the peraluminous composition melts do not enter the melt structure as viscosity reducing network modifiers, or as structures that result in the formation of more non-bridging O atoms. The most probable peraluminous melt structure is that discussed by Lacy (1963) and Toplis et al. (1997a, 1997b), in

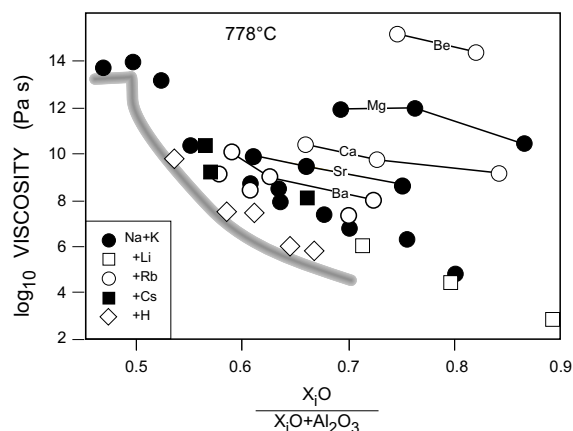


**FIGURE 9.** Viscosity of granitic composition melts at 778 °C as a function of alkali and alkaline earth content. The HPG8 composition (solid circles) has various amounts of  $\text{H}_2\text{O}$ ,  $\text{Li}_2\text{O}$ ,  $\text{Rb}_2\text{O}$ ,  $\text{Cs}_2\text{O}$ ,  $\text{BeO}$ ,  $\text{MgO}$ ,  $\text{CaO}$ ,  $\text{SrO}$ , and  $\text{BaO}$  added to it. The grey curve is that of Figure 4. Data from Hess et al. (1995, 1996) and Dingwell et al. (1996).

which tri-clusters of one O atom shared by two Si-tetrahedra and one Al-tetrahedron exist. This structural unit is charge-balanced and does not reduce the polymerization of the melt. The lack of change in viscosity with increasing Al-content together with the relatively constant activation energy for viscous flow with respect to that for the  $16.7\text{Na}_2\text{O} \cdot 16.7\text{Al}_2\text{O}_3 \cdot 66.7\text{SiO}_2$  composition suggests that the presence of an increasing number of tri-clusters does not affect the mechanism of flow in these melts.

Figure 4 also illustrates the reason for the different glass transition temperatures and viscosities for different "albite" compositions observed by Knoche et al. (1992). They observed a 100 °C decrease in  $T_g$  for albite composition melts with  $\text{Na}_2\text{O}/(\text{Na}_2\text{O} + \text{Al}_2\text{O}_3)$  of 48.8 and 51.8. The viscosity in Figure 4 is seen to decrease rapidly for slightly Na-rich compositions, but remain essentially constant for the Al-rich melts in the vicinity of the 1:1 join for Na and Al. The viscosity decrease from  $\text{Na}_2\text{O}/(\text{Na}_2\text{O} + \text{Al}_2\text{O}_3) = 0.49$  to 0.52 is approximately  $2.5 \log_{10} \text{Pa.s}$ , which is equivalent to a 100 °C change in temperature (see Table 2).

### ACKNOWLEDGMENTS

Thanks to U. Köhler, P. Meier, and A. Hampe for making the samples, and to M. Zimova and A. Kronz for the microprobe analyses. Thanks also to A. Navrotsky for useful discussions.

### REFERENCES CITED

- Brückner, R. and Demharter, G. (1975) Systematische Untersuchung über die Anwendbarkeit von Penetrationsviskosimetern. *Glastechnische Berichte*, 48, 12–18.
- Dingwell, D.B., Romano, C., and Hess, K.U. (1996) The effect of water on the viscosity of a haplogranitic melt under *P-T-X* conditions relevant to silicic volcanism. *Contributions to Mineralogy and Petrology*, 124, 19–28.
- Douglas, R.W., Armstrong, W.L., Edward, J.P., and Hall, D. (1965) A penetration viscometer. *Glass Technology*, 6, 52–55.
- Hess, K.U., Dingwell, D.B., and Webb, S.L. (1995) The influence of excess alkalis on the viscosity of a haplogranitic melt. *American Mineralogist*, 80, 297–304.
- Hess, K.U., Dingwell, D.B., and Webb, S.L. (1996) The influence of alkaline-earth oxides ( $\text{BeO}$ ,  $\text{MgO}$ ,  $\text{CaO}$ ,  $\text{SrO}$ ,  $\text{BaO}$ ) on the viscosity of a haplogranitic melt: systematics of non-Arrhenian behaviour. *European Journal of Mineralogy*, 8, 371–381.
- Hunold, K. and Brückner, R. (1980) Physikalische Eigenschaften und strukturelle Feinbau von Natrium-Aluminosilicatgläsern und -schmelzen. *Glastechnische Berichte*, 6S, 149–161.
- Knoche, R., Dingwell, D.B., and Webb, S.L. (1992) Non-linear temperature dependence of liquid volumes in the system albite-anorthite-diopside. *Contributions to Mineralogy and Petrology*, 111, 61–73.
- Lacy, E.D. (1963) Aluminium in glasses and in melts. *Physics and Chemistry of Glasses*, 4, 234–238.
- McMillan, P.F., Poe, B.T., Gillet, P., and Reynard, B. (1994) A study of  $\text{SiO}_2$  glass and supercooled liquid to 1950K via high temperature Raman spectroscopy. *Geochimica et Cosmochimica Acta*, 58, 3653–3664.
- Mysen, B.O., Virgo, D., and Kushiro, I. (1981) The structural role of aluminium in silicate melts—a Raman spectroscopic study at one atmosphere. *American Mineralogist*, 66, 678–701.
- Mysen, B.O. (1987) Magmatic silicate melts: Relationships between bulk composition, structure and properties. In B.O. Mysen, Ed., *Magmatic Processes: Physicochemical Principles*, Special Publication No. 1. The Geochemical Society, University Park, Pennsylvania.
- Mysen, B.O. (1988) *Structure and Properties of Silicate Melts: Developments in Geochemistry*, 4, Elsevier, Amsterdam.
- Poole, J.P. and Gensamer, M. (1949) Systematic Study of Effect of Oxide Constituents on Viscosity of Silicate Glasses at Annealing Temperatures. *Journal of the American Ceramic Society*, 32, 220–229.
- Riebling, E.F. (1966) Structure of sodium aluminosilicate melts containing at least 50 mol%  $\text{SiO}_2$  at 1500 °C. *Journal of Chemical Physics*, 44, 2857–2865.
- Riebling, E.F. (1968) Structural Similarities Between a Glass and Its Melt. *Journal of the American Ceramic Society*, 51, 143–1449.
- Stebbins, J.F. (1995) Dynamics and structure of silicate and oxide melts: Nuclear magnetic resonance studies. In J. Stebbins, P.F. McMillan, and D.B. Dingwell, Eds., *Structure, Dynamics and Properties of Silicate Melts*, 32, 191–246. Reviews in Mineralogy, Mineralogical Society of America, Washington, D.C.
- Stebbins, J.F. and Xu, Z. (1997) NMR evidence for excess non-bridging oxygen in an aluminosilicate glass. *Nature*, 390, 60–62.

- Stebbins, J.F., Zhao, P., Lee, S.K., and Ogelsby, J.V. (2001) Direct observation of multiple oxygen sites in oxide glasses: recent advances from triple-quantum magic-angle spinning nuclear magnetic resonance. *Journal of Non-Crystalline Solids*, 293, 67–73.
- Taylor, H.E. and Rindone, G.E. (1970) Properties of soda aluminosilicate glasses: V. low-temperature viscosities. *Journal of the American Ceramic Society*, 53, 692–695.
- Toplis, M.J. (1998) Energy barriers to viscous flow and the prediction of glass transition temperatures of molten silicates, *American Mineralogist*, 83, 480–490.
- Toplis, M.J., Dingwell, D.B., Hess, K.U., and Lenci, T. (1997a) Peraluminous viscosity maxima in  $\text{Na}_2\text{O}-\text{Al}_2\text{O}_3-\text{SiO}_2$  liquids: The role of triclusters in tectosilicate melts. *Geochimica et Cosmochimica Acta*, 61, 2605–2612.
- Toplis, M.J., Dingwell, D.B., Hess, K.-U., and Lenci, T. (1997b) Viscosity, fragility, and configurational entropy of melts along the join  $\text{SiO}_2-\text{NaAlSiO}_4$ . *American Mineralogist*, 82, 979–990.

MANUSCRIPT RECEIVED MAY 1, 2003

MANUSCRIPT ACCEPTED JANUARY 21, 2004

MANUSCRIPT HANDLED BY DONALD DINGWELL